
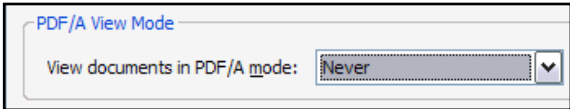
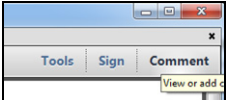
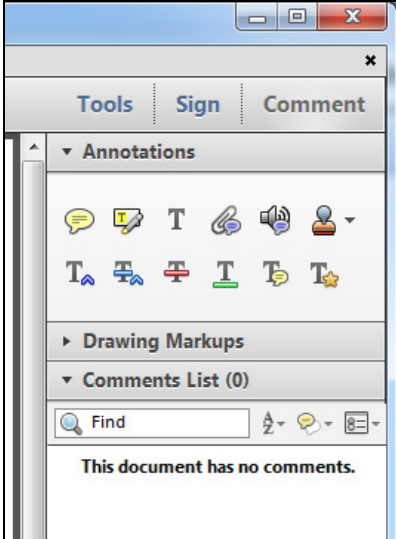


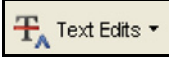


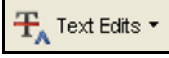

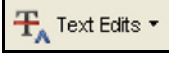






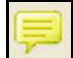
INSTRUCTIONS ON THE ANNOTATION OF PDF FILES

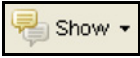
To view, print and annotate your article you will need Adobe Reader version 9 (or higher). This program is freely available for a whole series of platforms that include PC, Mac, and UNIX and can be downloaded from <http://get.adobe.com/reader/>. The exact system requirements are given at the Adobe site: <http://www.adobe.com/products/reader/tech-specs.html>.

Note: if you opt to annotate the file with software other than Adobe Reader then please also highlight the appropriate place in the PDF file.

PDF ANNOTATIONS	
Adobe Reader version 9	Adobe Reader version X and XI
<p>When you open the PDF file using Adobe Reader, the Commenting tool bar should be displayed automatically; if not, click on 'Tools', select 'Comment & Markup', then click on 'Show Comment & Markup tool bar' (or 'Show Commenting bar' on the Mac). If these options are not available in your Adobe Reader menus then it is possible that your Adobe Acrobat version is lower than 9 or the PDF has not been prepared properly.</p>  <p>(Mac)</p> <p>PDF ANNOTATIONS (Adobe Reader version 9)</p> <p>The default for the Commenting tool bar is set to 'off' in version 9. To change this setting select 'Edit Preferences', then 'Documents' (at left under 'Categories'), then select the option 'Never' for 'PDF/A View Mode'.</p>  <p>(Changing the default setting, Adobe version 9)</p>	<p>To make annotations in the PDF file, open the PDF file using Adobe Reader XI, click on 'Comment'.</p> <p>If this option is not available in your Adobe Reader menus then it is possible that your Adobe Acrobat version is lower than XI or the PDF has not been prepared properly.</p>  <p>This opens a task pane and, below that, a list of all Comments in the text. These comments initially show all the changes made by our copyeditor to your file.</p> 

HOW TO...

Action	Adobe Reader version 9	Adobe Reader version X and XI
Insert text	Click the 'Text Edits' button  on the Commenting tool bar. Click to set the cursor location in the text and simply start typing. The text will appear in a commenting box. You may also cut-and-paste text from another file into the commenting box. Close the box by clicking on 'x' in the top right-hand corner.	Click the 'Insert Text' icon  on the Comment tool bar. Click to set the cursor location in the text and simply start typing. The text will appear in a commenting box. You may also cut-and-paste text from another file into the commenting box. Close the box by clicking on '_'  in the top right-hand corner.
Replace text	Click the 'Text Edits' button  on the Commenting tool bar. To highlight the text to be replaced, click and drag the cursor over the text. Then simply type in the replacement text. The replacement text will appear in a commenting box. You may also cut-and-paste text from another file into this box. To replace formatted text (an equation for example) please Attach a file (see below).	Click the 'Replace (Ins)' icon  on the Comment tool bar. To highlight the text to be replaced, click and drag the cursor over the text. Then simply type in the replacement text. The replacement text will appear in a commenting box. You may also cut-and-paste text from another file into this box. To replace formatted text (an equation for example) please Attach a file (see below).
Remove text	Click the 'Text Edits' button  on the Commenting tool bar. Click and drag over the text to be deleted. Then press the delete button on your keyboard. The text to be deleted will then be struck through.	Click the 'Strikethrough (Del)' icon  on the Comment tool bar. Click and drag over the text to be deleted. Then press the delete button on your keyboard. The text to be deleted will then be struck through.
Highlight text/ make a comment	Click on the 'Highlight' button  on the Commenting tool bar. Click and drag over the text. To make a comment, double click on the highlighted text and simply start typing.	Click on the 'Highlight Text' icon  on the Comment tool bar. Click and drag over the text. To make a comment, double click on the highlighted text and simply start typing.
Attach a file	Click on the 'Attach a File' button  on the Commenting tool bar. Click on the figure, table or formatted text to be replaced. A window will automatically open allowing you to attach the file. To make a comment, go to 'General' in the 'Properties' window, and then 'Description'. A graphic will appear in the PDF file indicating the insertion of a file.	Click on the 'Attach File' icon  on the Comment tool bar. Click on the figure, table or formatted text to be replaced. A window will automatically open allowing you to attach the file. A graphic will appear indicating the insertion of a file.
Leave a note/ comment	Click on the 'Note Tool' button  on the Commenting tool bar. Click to set the location of the note on the document and simply start typing. <u>Do not use this feature to make text edits.</u>	Click on the 'Add Sticky Note' icon  on the Comment tool bar. Click to set the location of the note on the document and simply start typing. <u>Do not use this feature to make text edits.</u>

HOW TO...		
Action	Adobe Reader version 9	Adobe Reader version X and XI
Review	To review your changes, click on the 'Show' button  on the Commenting tool bar. Choose 'Show Comments List'. Navigate by clicking on a correction in the list. Alternatively, double click on any mark-up to open the commenting box.	Your changes will appear automatically in a list below the Comment tool bar. Navigate by clicking on a correction in the list. Alternatively, double click on any mark-up to open the commenting box.
Undo/delete change	To undo any changes made, use the right click button on your mouse (for PCs, Ctrl-Click for the Mac). Alternatively click on 'Edit' in the main Adobe menu and then 'Undo'. You can also delete edits using the right click (Ctrl-click on the Mac) and selecting 'Delete'.	To undo any changes made, use the right click button on your mouse (for PCs, Ctrl-Click for the Mac). Alternatively click on 'Edit' in the main Adobe menu and then 'Undo'. You can also delete edits using the right click (Ctrl-click on the Mac) and selecting 'Delete'.


SEND YOUR ANNOTATED PDF FILE BACK TO ELSEVIER

Save the annotations to your file and return as instructed by Elsevier. Before returning, please ensure you have answered any questions raised on the Query Form and that you have inserted all corrections: later inclusion of any subsequent corrections cannot be guaranteed.

FURTHER POINTS

- Any (grey) halftones (photographs, micrographs, etc.) are best viewed on screen, for which they are optimized, and your local printer may not be able to output the greys correctly.
- If the PDF files contain colour images, and if you do have a local colour printer available, then it will be likely that you will not be able to correctly reproduce the colours on it, as local variations can occur.
- If you print the PDF file attached, and notice some 'non-standard' output, please check if the problem is also present on screen. If the correct printer driver for your printer is not installed on your PC, the printed output will be distorted.

AUTHOR QUERY FORM

 ELSEVIER	Journal: YMVA Article Number: 8141	Please e-mail your responses and any corrections to: E-mail: a.obrien@elsevier.com
------------------------------------------------------------------------------------------------------	---------------------------------------------------------	----------------------------------------------------------------------------------------------------------------------------------------------------

Dear Author,

Please check your proof carefully and mark all corrections at the appropriate place in the proof (e.g., by using on-screen annotation in the PDF file) or compile them in a separate list. Note: if you opt to annotate the file with software other than Adobe Reader then please also highlight the appropriate place in the PDF file. To ensure fast publication of your paper please return your corrections within 48 hours.

For correction or revision of any artwork, please consult <http://www.elsevier.com/artworkinstructions>.

Any queries or remarks that have arisen during the processing of your manuscript are listed below and highlighted by flags in the proof.

Location in article	Query / Remark: Click on the Q link to find the query's location in text Please insert your reply or correction at the corresponding line in the proof
<p>Q1</p> <p>Q2</p>	<p>If there are any drug dosages in your article, please verify them and indicate that you have done so by initialing this query</p> <p>Please provide the professional degree for author “Daniele Mariastefano Fontanini.”</p> <p>Author affiliations will appear differently in the print and online versions of your paper. The PDF shows how the affiliations will present following journal style, whereas the searchable online version will present as follows in order to provide complete unabridged affiliations. Please check the accuracy of the affiliation(s) of each author and make changes as appropriate.</p> <p>^aDepartment of Vascular Surgery, Heart and Vascular Center, Semmelweis University, Budapest, Hungary</p> <p>^bDepartment of Geometry, Budapest University of Technology and Economics, Budapest, Hungary</p> <p>^cMTA-SE Lendület Cardiovascular Imaging Research Group, Heart and Vascular Center, Semmelweis University, Budapest, Hungary.</p>
<p>Q3</p>	<p>Please confirm that given names and surnames have been identified correctly.</p> <div data-bbox="304 1506 895 1683" style="border: 1px solid black; padding: 10px;"> <p>Please check this box or indicate your approval if you have no corrections to make to the PDF file</p> <div style="text-align: right; margin-right: 20px;"> <input data-bbox="791 1570 874 1647" type="checkbox"/> </div> </div>

Thank you for your assistance.

Thoracic aortic strain can affect endograft sizing in young patients

Names are OK

03

Csaba Csobay-Novák, MD,^a Daniele Mariastefano Fontanini,^a Brigitta R. Szilágyi, PhD,^b

01

Zoltán Szeberin, MD, PhD,^a Bálint A. Szilveszter, MD,^c Pál Maurovich-Horvat, MD, PhD,^c

01

Kálmán Hüttl, MD, PhD,^a and Péter Sótónyi, MD, PhD,^a Budapest, Hungary

Fontanini DM is a university student, does not have a degree yet

Objective: Aortic computed tomography angiography (CTA) examination with electrocardiography gating is becoming the clinical routine image acquisition protocol for diagnosis and intervention planning. To minimize motion artifact, the images are reconstructed in the diastolic phase of the cardiac cycle. The aim of our study was to quantify aortic strain in an elderly nonaneurysmatic patient cohort and to identify the phases of the R-R cycle that correspond to the minimal and maximal aortic diameters. The quantification of aortic strain may enable the improvement of intervention planning and the introduction of more effective dose-saving protocols for CTA scans.

Methods: We assessed CTA images of 28 patients (14 men; mean age, 74 years). Aortic calcium score was calculated on native images. Angiography images were reconstructed in equally spaced 10 phases of the R-R cycle. After semiautomatic centerline analysis, we measured the cross-sectional areas in each of the 10 phases at 9 specific segments between the ascending aorta and the common iliac bifurcation representing the attachment sites of thoracic and abdominal stent grafts. Area-derived effective diameter, pulsatility ($A_{\max} - A_{\min}$), and strain $[(A_{\max} - A_{\min})/A_{\min}]$ were calculated. Repeated measurements were taken to evaluate inter-reader and intrareader reproducibility (10-10 patients each).

Results: A total of 4320 measurements were performed. We found significant difference between diastolic and systolic diameters ($D_{D,Z0} = 33.2$, $D_{S,Z0} = 34.4$; $P < .001$). Pulsatility values of the vessel diameters were 1.0 to 1.1 mm in the thoracic aorta, 0.7 to 0.9 mm in the abdominal aorta, and 0.5 to 0.6 mm in the common iliac arteries. Negative, moderate correlations were found between aortic strain and age ($r = -0.586$; $P = .001$), aortic strain and plaque area ($r = -0.429$; $P = .026$), and age and body mass index ($r = -0.412$; $P = .029$). We found positive, moderate correlation between age and plaque area ($r = 0.594$; $P = .001$). The aortic pulsatility curve has a positive extreme at 30% and a negative extreme at 90% of the R-R cycle throughout the aorta. Lin concordance coefficients were 0.987 for inter-reader and 0.994 for intrareader correlations.

Conclusions: Aortic strain can be reliably quantified on electrocardiography-gated CTA images. Pulsatility of the aorta can be substantial in the thoracic aortic segments of young patients; therefore, the routine use of systolic images is not recommended. In addition, we demonstrated that images at 30% of the heart cycle correspond to the largest diameter of the aorta. (J Vasc Surg 2015;■:1-6.)

There is growing evidence that endovascular aortic repair (EVAR) can be safely and effectively performed in thoracic and abdominal aortic diseases, such as aortic aneurysm and acute aortic syndrome.¹⁻⁵ Simultaneously, a shift in the last 15 years can be observed from open repair to EVAR; however, there is an ongoing debate as to whether we should push the boundaries too far in favor of EVAR.⁶ Thoracic and abdominal EVAR is associated with lower mortality rates compared with open repair, but there is a non-negligible number of EVAR patients who suffer late

complications of the stent grafts caused by migration and endoleaks.⁷⁻⁹ As both undersizing and excessive oversizing are known to be associated with complications in the short and long term, precise sizing of the stent graft is crucial.^{8,10,11}

Previous generations of computed tomography (CT) scanners with a lower number of detector rows and slower gantry rotation without electrocardiography (ECG) synchronization produced images with a blurred aortic contour and a somewhat averaged aortic diameter because of aortic wall motion. Nowadays, technologic advances allow rapid ECG-gated CT angiography (CTA) of the whole aorta during a single breath-hold, confronting us with new problems: which phase of the cardiac cycle should be used for image acquisition or reconstruction?¹² Conventionally, diastolic images are preferred as systolic images are often compromised by motion artifacts. However, aortic diameter changes during the R-R cycle can be substantial, especially in the young; wavy aortic contour on pediatric CT images is a usual finding. If the systolic-diastolic difference of the aortic diameter is considerable, this can result in an undersized stent graft.¹²

In this study, our primary objective was to measure the strain of the whole aorta on ECG-gated CTA images in an

Affiliations are OK

From the Department of Vascular Surgery^a and MTA-SE Lendület Cardiovascular Imaging Research Group,^c Heart and Vascular Center, Semmelweis University; and the Department of Geometry, Budapest University of Technology and Economics.^b

Author conflict of interest: none.

Correspondence: Csaba Csobay-Novák, MD, Department of Vascular Surgery, Heart and Vascular Center, Semmelweis University, Határőr út 18, Budapest, H-1122, Hungary (e-mail: media@csobay.hu).

The editors and reviewers of this article have no relevant financial relationships to disclose per the JVS policy that requires reviewers to decline review of any manuscript for which they may have a conflict of interest.

0741-5214

Copyright © 2015 by the Society for Vascular Surgery. Published by Elsevier Inc.

<http://dx.doi.org/10.1016/j.jvs.2015.06.225>

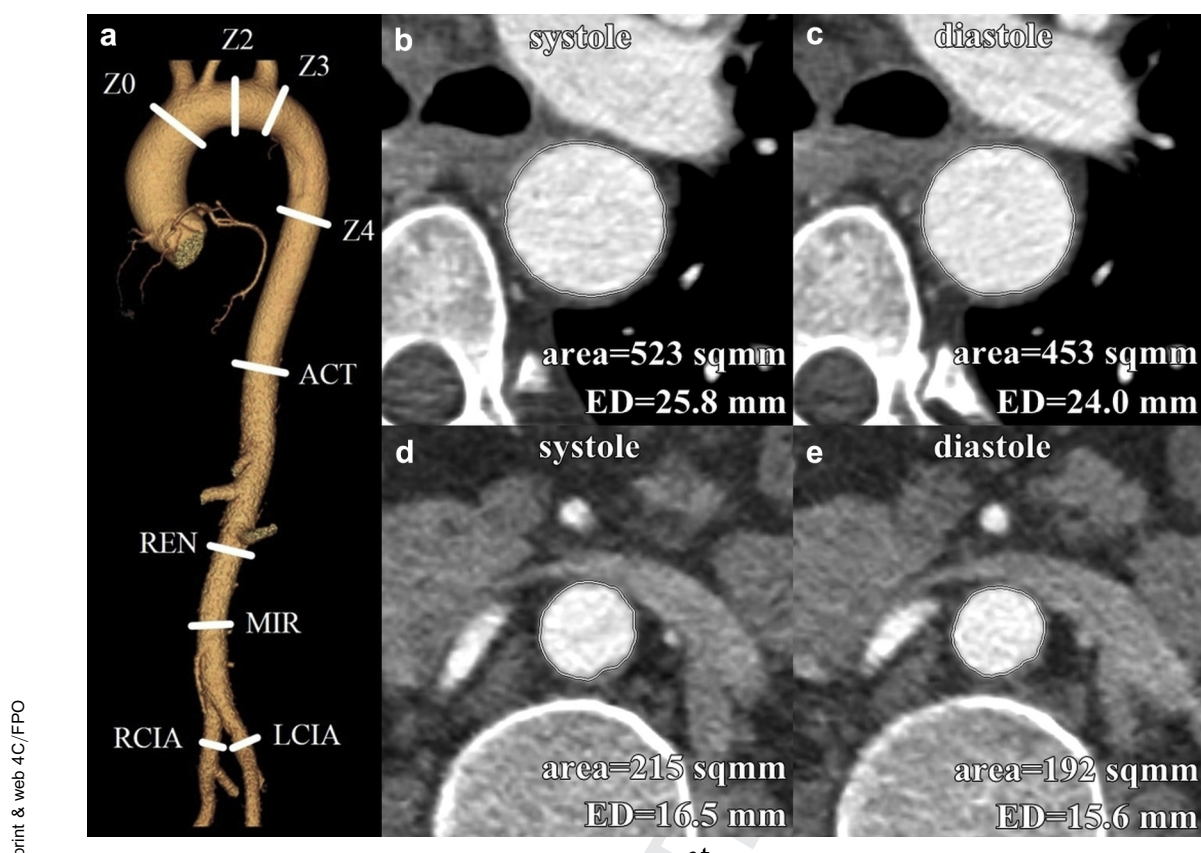


Fig 1. a, Locations of cross-sectional area measurements. ACT, at 5 cm above celiac trunk origin; LCIA, left common iliac artery; MIR, middle infrarenal aorta; RCIA, right common iliac artery; REN, below renal ostia; Z0, Z2, Z3, Z4, Ishimaru zones of the thoracic aorta. b to e, Systolic and diastolic phase cross-sectional images perpendicular to the centerline at the level of Z4 (b and c) and REN (d and e). ED, Area-derived effective diameter.

elderly patient cohort with atherosclerotic but otherwise normal aorta. Our secondary objective was to identify the phases of the R-R cycle that correspond to the maximal (systolic) and minimal (diastolic) diameters, enabling us to introduce dose-saving options for CTA scans of future patients.

METHODS

CT imaging. Imaging of the aorta was performed in 28 patients (14 men; mean age, 72.9 ± 12.0 years) with a 256-slice multidetector CT scanner (Philips Brilliance iCT; Koninklijke Philips N.V., Best, The Netherlands) using an ECG-gated protocol tailored for imaging of the aorta. The study was performed on images readily available from patients being evaluated for transcatheter aortic valve repair (TAVR) or from patients with suspected acute aortic syndrome.

Hemodynamic parameters were measured with an electronic sphygmomanometer before administration of contrast material. A low-dose (tube voltage, 100 kV) native scan was followed by retrospective ECG-gated CTA of the whole aorta (100 kV) with a reduced field of view to maximize spatial resolution. Nonionic contrast agent was

injected into an antecubital vein at a flow rate of 4 to 5 mL/s using a power injector. Images were reconstructed using a sharp convolution kernel and iterative reconstruction algorithm (iDose,⁴ Koninklijke Philips N.V.) with a slice thickness of 1 mm and an increment of 1 mm. Multi-phase images were reconstructed corresponding to every 10% of the R-R cycle, resulting in 10 series of images for each patient. Data sets were transferred to stand-alone workstations for further analysis.

Image analysis. Image analysis, vessel segmentation, and cross-sectional measurements were performed by two independent radiologists experienced in cardiovascular imaging. Aortic calcifications were calculated using the dedicated coronary calcium scoring software of an Extended Brilliance Workspace (HeartBeat CS, Koninklijke Philips N.V.).

CTA images were analyzed using an Advantage Workstation (GE Healthcare Europe GmbH, Freiburg, Germany). After automatic vessel segmentation and centerline detection, cross-sectional area of the lumen was measured in a semiautomatic fashion at the following nine locations: ascending aorta proximal to the brachiocephalic trunk (Ishimaru Z0), between left common carotid

Doesn't have to be numbered, as it is the only table?

Table. Demographic and procedural data

Patient characteristics	N = 28
Age, years	74 (64-82)
Male gender	14 (50)
Body mass index, kg/m ²	25 (23-27)
Previous myocardial infarction	8 (29)
Previous stroke	4 (14)
Hypertension	26 (93)
Hyperlipidemia	13 (46)
Diabetes mellitus	4 (14)
Smoking history	7 (25)
Systolic blood pressure, mm Hg	132 (116-162)
Diastolic blood pressure, mm Hg	76 (65-86)
Pulse pressure, mm Hg	57 (46-78)
Heart rate, beats/min	71 (60-82)
Dose-length product, mGy-cm	2197 (1194-2604)
Aortic plaque area	2777 (846-4996)

Continuous data are presented as median (interquartile range); categorical data are number (percentage).

artery and left subclavian artery (Ishimaru Z2), immediately distal to the left subclavian artery (Ishimaru Z3), 5 cm distal to the left subclavian artery (Ishimaru Z4), 5 cm above celiac trunk ostium, below renal ostia, middle infrarenal aorta, and right and left common iliac artery (Fig 1, a).^{13,14} Position was matched in three dimensions between series of different phases by recording the slice number that involved the segment of the centerline at the exact point of the measurements taken. Cross-sectional areas were recorded in square millimeters. Diameter was calculated as the diameter of a virtual circle with the same cross-sectional area (area-derived effective diameter; Fig 1, b-e). To minimize measurement errors and to increase inter-reader agreement, direct diameter measurements were avoided.¹² Pulsatility was defined as the largest difference between systolic maximum and diastolic minimum diameter or area. Vessel strain was calculated as a ratio of pulsatility and minimum area $[(A_{\max} - A_{\min})/A_{\min}]$. Patients gave written informed consent before CT examination was performed. The experimental protocol and informed consent were approved by the Regional Ethical Committee of Semmelweis University (133/2011).

Statistical analysis. Data processing and analysis were performed using IBM SPSS Statistics 22.0 (IBM Corporation, Armonk, NY) and R (R Foundation for Statistical Computing, Vienna, Austria) software. Shapiro-Wilk test was used to assess the normality of the data. Wilcoxon signed rank test was used to compare diastolic and systolic measurements. Correlations were analyzed with Spearman ρ test. Lin correlation was used to evaluate inter-reader and intrareader agreement.¹⁵ Statistically significant difference was established at $P < .05$. Continuous variables are presented as median (interquartile range).

RESULTS

A total of 4320 measurements on 28 patients were performed, involving 1800 repeated measurements on 20

patients to evaluate inter-reader and intrareader reproducibility. Patient demographics are shown in Table.

Wilcoxon signed rank test showed significant difference between the cross-sectional areas of the diastolic and systolic phases ($P < .001$) at every anatomic location measured.

Area pulsatility is reduced along the course of the aorta; the highest level was measured at the Z0 position (42.9 mm² [28.8-74.0 mm²]) with a continuous decrease along the aorta to an almost negligible value at the level of the iliac arteries (8.5 mm² [6-12 mm²]). This equals a diameter pulsatility of 1.0 mm (0.6-1.6 mm) at the thoracic aorta (Z0), 0.7 mm (0.6-1.0 mm) at the abdominal aorta (below renal ostia), and 0.5 mm (0.4-0.8 mm) at the common iliac arteries (Fig 2, a). As vessel diameter is decreasing more rapidly than pulsatility (Fig 2, b), vessel strain is somewhat higher in the infradiaphragmatic segments but does not reach the level of significance; 3% to 5% was found throughout the aorta with wide interquartile ranges (Fig 2, c).

To identify the positive and negative extremes in the R-R cycle of aortic pulsatility, we derived a parameter representing the precession of the actual diameter relative to the mean diameter $[(d_{\text{actual}} - d_{\text{mean}})/d_{\text{mean}}]$. This resulted in a graph resembling an arterial pressure curve, with a systolic extreme at 30% and a diastolic extreme at 90% of the R-R cycle (Fig 2, d).

Lin concordance coefficients were 0.987 for inter-reader (range, 0.985-0.991; strength of agreement: substantial) and 0.994 for intrareader (range, 0.993-0.995; strength of agreement: almost perfect) correlations.¹⁵ A higher inter-reader variability was found between iliac artery measurements (concordance coefficients were 0.831 for right common iliac artery and 0.267 for left common iliac artery; strength of agreement: poor). Therefore, iliac artery measurements were excluded from correlation analysis.

Negative correlations were found between aortic strain and age ($r = -0.498$, $P = .007$ at Z3; $r = -0.586$, $P = .001$ at Z4; $r = -0.539$, $P = .003$ at 5 cm above celiac trunk ostium), aortic strain and plaque area ($r = -0.429$, $P = .026$ at Z4; $r = -0.436$, $P = .023$ at 5 cm above celiac trunk ostium), and age and body mass index ($r = -0.412$; $P = .029$). Positive correlation between age and plaque area ($r = 0.594$; $P = .001$) was found. Pulse pressure did not show any significant correlation with the other parameters.

DISCUSSION

This study was undertaken to evaluate the strain of the vessel segments commonly used as landing zones of aortic stent grafts on CTA images. A previous work conducted by Parodi et al¹² examined the proximal segment of the descending aorta of 27 patients. They found significant difference between systolic and diastolic diameters at 1, 4, and 8 cm distal to the left subclavian artery, thus concluding that the use of diastolic images for stent graft planning can result in undersizing and possible complications.

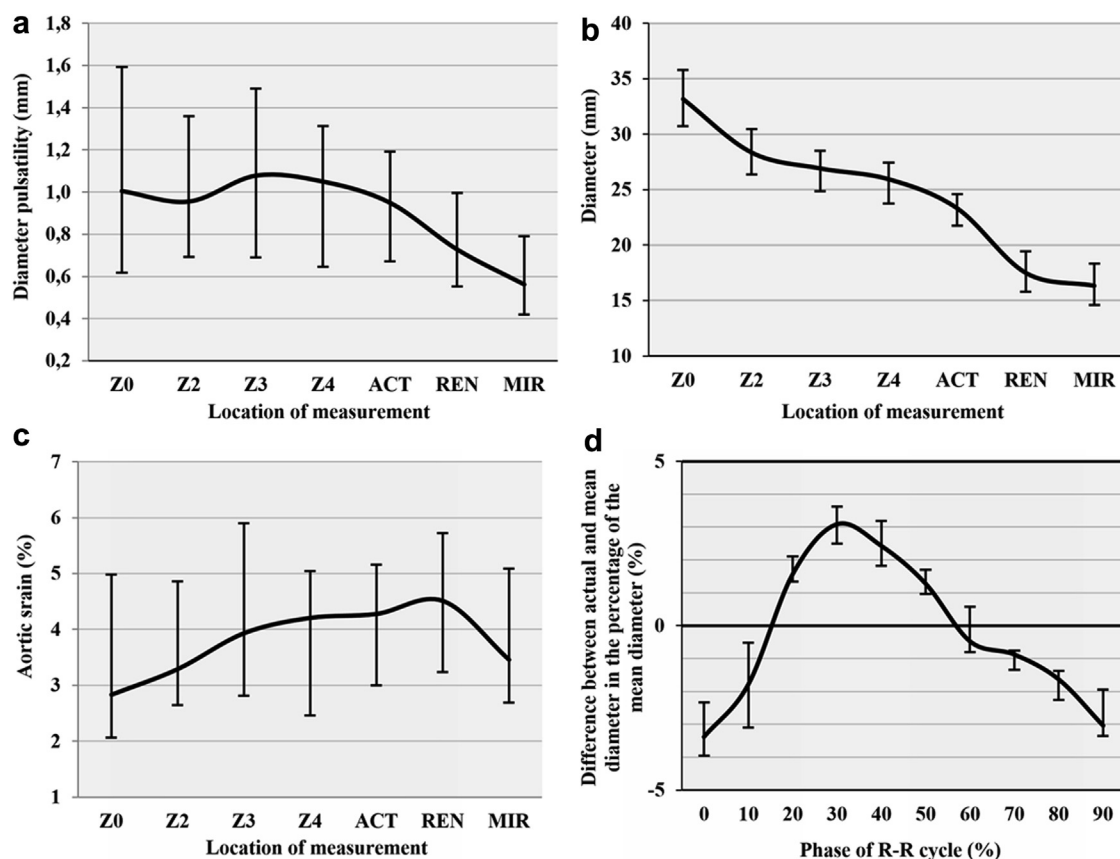


Fig 2. Geometric parameters of the aorta: (a) diameter pulsatility; (b) diameter; (c) strain; (d) difference between actual and mean diameter in the percentage of the mean diameter. Data are presented as medians with interquartile ranges. *ACT*, At 5 cm above celiac trunk origin; *MIR*, middle infrarenal aorta; *REN*, below renal ostia; *Z0*, *Z2*, *Z3*, *Z4*, Ishimaru zones of the thoracic aorta.

Our results refine these findings, as 75% of the patients had a diameter pulsatility of <1.5 mm in the thoracic aorta. This questions the need for systolic images in thoracic stent graft planning.

The magnitude of pulsatility is reduced with the distal tapering and branching of the aorta, being <1 mm in the abdominal aorta and iliac vessels in the majority of the patients, which questions its relevance regarding the sizing of infradiaphragmatic prostheses. On the basis of our findings, neither three-dimensional motion nor pulsatility of these vessels is notable; thus, the routine use of ECG gating for abdominal CTA examinations is not recommended unless it does not increase radiation dose and contrast agent volume (prospective ECG-triggered, high-pitch helical acquisition is available on some of the latest scanners only).

The wide distribution of the samples of aortic strain measurements can most likely be addressed by the heterogeneity of our patient cohort. There are data that aortic strain reduces with advancing age. Previous studies show that thoracic aortic strain in a young adult can be as high as 33%, with a nonlinear decrease with advancing age; 80% of the total decline of aortic strain occurs before the fifth decade.^{16,17} The significant

negative correlation in our elderly and small patient cohort between aortic strain and age emphasizes the importance of using systolic images in young patients. Young patients are at the highest risk of suffering an involuntary undersizing of an aortic stent graft due to the use of diastolic images. This risk is further increased by the progressive dilation of the aorta with age, which is in the range of 1.5 mm per 10 years according to literature data.¹⁶

The higher inter-reader variability found between iliac artery measurements can be addressed by the following three causes: (1) possible anatomic mismatch between the different phases due to vessel tortuosity; (2) smaller diameter of the vessels; and (3) extensive blooming artifacts caused by the calcification of the common iliac arteries, making edge detection more difficult.

We found significant negative correlation between aortic strain and plaque area; however, it is not clear whether calcification itself has a role in the increase of wall stiffness. Previous research suggests that alterations in cellular and extracellular components of the vessel wall appear in young adulthood, causing alterations in mechanical properties of the vessel wall preceding calcification.¹⁶

To reduce the effective dose of future patients needing aortic imaging, identification of positive (systolic) and negative (diastolic) extremes of the aortic diameter during the R-R cycle was necessary. Dose-saving methods such as prospective ECG triggering or ECG-dependent tube current modulation must be used to maximize image quality at 30%. With the limited temporal resolution of today's CT technology, accurate assessment of temporal shifts of the curves between different vessel segments is barely possible and most likely irrelevant regarding stent graft planning.

A possible role of ECG-gated CTA imaging in the evaluation of aneurysmatic disease progression, rupture risk estimation, and prediction of proximal neck dilation has been raised by several authors.^{18,19} Local vessel parameters can be derived from aortic strain: pressure strain elastic modulus and vessel distensibility. A major drawback of these parameters is the need of blood pressure values, as continuous invasive blood pressure recording is usually not possible during image acquisition. Measuring blood pressure levels before or after injection of contrast material causes an unpredictable error, as inspirational breath-hold and Valsalva maneuver can have major effects on the short-term regulation of hemodynamic parameters. Novel mechanical parameters derived by others show a promising result in the understanding and quantification of the local properties of the healthy and diseased aorta.^{18,19} Finding a new parameter that can be derived from widely available CTA images and that could estimate disease progression would be a game changer for patients with aortic disease.

Study limitations. Inclusion of TAVR candidates raises questions, as these patients may have abnormal pulse pressures due to aortic valve stenosis or insufficiency. There were no significant correlations between pulsatility or strain and aortic pulse pressure, nor significant difference in aortic strain between TAVR and not TAVR patients.

The three-dimensional motion of the aorta can result in a mismatch between the phases of the R-R cycle in the same cross sections of the measured segments. Measurement locations were anchored to the table position and slice number, as a reliable anatomic landmark of the aortic wall was not present in every location. However, aortic motion is usually <1 mm. Heterogeneity of aortic strain resulting in significant difference between the phases is not likely.

All of our patients were nonaneurysmatic patients, whereas the majority of aortic interventions are planned to treat aortic aneurysms. We believe that our recommendations based on our nonaneurysmatic cohort can be beneficial for aneurysmatic patients also. However, further investigations are needed to evaluate the interindividual and intraindividual differences in aortic pulsatility and strain in aneurysmatic disease.

CONCLUSIONS

Aortic strain can be measured on ECG-gated CTA images with high reliability and reproducibility. The aortic pulsatility was <1 mm in the abdominal aorta

and <1.5 mm in the thoracic aorta in the majority of the patients; therefore, the routine use of systolic images cannot be justified. In most cases, nongated CTA is appropriate for device selection if descending thoracic or abdominal aortic disease is present. However, a subgroup of younger patients might exist in whom aortic strain can reach the level of significance.

Novel mechanical parameters derived from dynamic cross-sectional images may have a future role in estimating disease progression as they can be accurately measured on routine CTA scans.

AUTHOR CONTRIBUTIONS

Conception and design: CC, DF, BRS, ZS, BAS, PM, KH, PS
Analysis and interpretation: CC, DF, BRS, BAS, PM, PS
Data collection: CC, DF, BRS, BAS
Writing the article: CC, DF, BRS, BAS, PM, KH, PS
Critical revision of the article: CC, DF, BRS, ZS, BAS, PM, KH, PS
Final approval of the article: CC, ZS, KH, PS
Statistical analysis: CC, BRS, BAS, PS
Obtained funding: Not applicable
Overall responsibility: CC

REFERENCES

- Najibi S, Terramani TT, Weiss VJ, Mac Donald MJ, Lin PH, Redd DC, et al. Endoluminal versus open treatment of descending thoracic aortic aneurysms. *J Vasc Surg* 2002;36:732-7.
- Leurs LJ, Bell R, Degrieck Y, Thomas S, Hobo R, Lundbom J. Endovascular treatment of thoracic aortic diseases: combined experience from the EUROSTAR and United Kingdom Thoracic Endograft registries. *J Vasc Surg* 2004;40:670-9; discussion: 679-80.
- Makaroun MS, Dillavou ED, Kee ST, Sicard G, Chaikof E, Bavaria J, et al. Endovascular treatment of thoracic aortic aneurysms: results of the phase II multicenter trial of the GORE TAG thoracic endoprosthesis. *J Vasc Surg* 2005;41:1-9.
- Bavaria JE, Appoo JJ, Makaroun MS, Verter J, Yu ZF, Mitchell RS. Endovascular stent grafting versus open surgical repair of descending thoracic aortic aneurysms in low-risk patients: a multicenter comparative trial. *J Thorac Cardiovasc Surg* 2007;133:369-77.
- Matsumura JS, Cambria RP, Dake MD, Moore RD, Svensson LG, Snyder S. International controlled clinical trial of thoracic endovascular aneurysm repair with the Zenith TX2 endovascular graft: 1-year results. *J Vasc Surg* 2008;47:247-57; discussion: 257.
- Clagett GP. EVAR, TEVAR, FEVAR, too far? *Perspect Vasc Surg Endovasc Ther* 2008;20:115-9.
- Stone DH, Brewster DC, Kwolek CJ, Lamuraglia GM, Conrad MF, Chung TK, et al. Stent-graft versus open-surgical repair of the thoracic aorta: mid-term results. *J Vasc Surg* 2006;44:1188-97.
- Sternbergh WC 3rd, Money SR, Greenberg RK, Chuter TA. Influence of endograft oversizing on device migration, endoleak, aneurysm shrinkage, and aortic neck dilation: results from the Zenith Multicenter Trial. *J Vasc Surg* 2004;39:20-6.
- Parmer SS, Carpenter JP, Stavropoulos SW, Fairman RM, Pochettino A, Woo EY, et al. Endoleaks after endovascular repair of thoracic aortic aneurysms. *J Vasc Surg* 2006;44:447-52.
- Iezzi R, Santoro M, Di Natale G, Pirro F, Dattesi R, Nestola M, et al. Aortic-neck dilation after endovascular abdominal aortic aneurysm repair (EVAR): can it be predicted? *Radiol Med* 2012;117:804-14.
- Erbel R, Aboyans V, Boileau C, Bossone E, Bartolomeo RD, Eggebrecht H, et al. 2014 ESC Guidelines on the diagnosis and treatment of aortic diseases: document covering acute and chronic

- 581 aortic diseases of the thoracic and abdominal aorta of the adult. The
582 Task Force for the Diagnosis and Treatment of Aortic Diseases of the
583 European Society of Cardiology (ESC). *Eur Heart J* 2014;35:
584 2873-926.
12. Parodi J, Berguer R, Carrascosa P, Khafer K, Capunay C, Wizauer E.
585 Sources of error in the measurement of aortic diameter in computed
586 tomography scans. *J Vasc Surg* 2014;59:74-9.
13. Ishimaru S. [Endovascular stent-graft repair for thoracic aortic aneurysm]. *Kyobu Geka* 2006;59(Suppl):666-73.
14. Ishimaru S. Endografting of the aortic arch. *J Endovasc Ther* 2004;11(Suppl 2):II62-71.
15. Lin LI. A concordance correlation coefficient to evaluate reproducibility. *Biometrics* 1989;45:255-68.
16. Redheuil A, Yu WC, Wu CO, Mousseaux E, de Cesare A, Yan R, et al. 594
595 Reduced ascending aortic strain and distensibility: earliest manifesta-
596 tions of vascular aging in humans. *Hypertension* 2010;55:319-26.
17. AlGhatrif M, Lakatta EG. The conundrum of arterial stiffness, elevated 597
598 blood pressure, and aging. *Curr Hypertens Rep* 2015;17:523.
18. Satriano A, Rivolo S, Martufi G, Finol EA, Di Martino ES. In vivo 599
600 strain assessment of the abdominal aortic aneurysm. *J Biomech*
601 2015;48:354-60.
19. Tierney AP, Callanan A, McGloughlin TM. Use of regional mechanical 602
603 properties of abdominal aortic aneurysms to advance finite element
604 modeling of rupture risk. *J Endovasc Ther* 2012;19:100-14.
- Submitted May 2, 2015; accepted Jun 29, 2015. 605
606